Synthesis of ZnO-loaded $Co_{0.85}Se$ nanocomposites and their enhanced performance for decomposition of hydrazine hydrate and catalytic hydrogenation of p-nitrophenol

Ting-Ting Xu＃, Jie Zhang＃, Ji-Ming Song,* He-Lin Niu, Chang-Jie Mao, Sheng-Yi Zhang, and Yu-Hua Shen

The Key Laboratory of Environment Friendly Polymer Materials of Anhui Province, School of Chemistry & Chemical Engineering, Anhui University, Hefei, Anhui, 230601, P. R. China.

Tel*:+86 0551 63861279* : Fax*: +86 0551 63861279*

E-mail: jiming@ahu.edu.cn

[＃] Xu and Zhang contribute equally to this article.

Abstract

Nanocomposite is a kind of multiphase solid materials with nano-dimensional. It generally displays more preferable performance than its corresponding single precursors or conventional composite materials due to size effect and interfacial effect. Herein, we report the synthesis of a kind of nanocomposite via one pot route without using any surfactant or structure-directing agents. The structure, composition and morphology of the as-synthesized products were characterized by XRD, XPS, SEM, TEM and BET surface area measurements. The results revealed that the prepared nanocomposites were consisted of ZnO-loaded $Co_{0.85}Se$ nanocomposites. BET measurement showed the specific surface area of the nanocomposite was 66.5 $m^2 g^{-1}$ at 77.5 K. Interestingly, the ZnO-loaded $Co_{0.85}Se$ nanocomposites exhibit remarkable performance for the decomposition of hydrazine hydrate and catalytic hydrogenation of p-nitrophenol compared with individual component of $Co_{0.85}Se$ or ZnO. More importantly, the obtained nanocomposites have very excellent stability and reversibility as catalysts, indicating that the products can be potentially used in wastewater treatment.

Keywords: ZnO; $Co_{0.85}Se$; nanocomposites; catalyst; hydrazine hydrate; p-nitrophenol

1. Introduction

Oxide semiconductor materials have attracted enormous attention in recent years, owing to their extensive application in various fields [1-3]. ZnO, as one of the most important oxide semiconductor materials with a wide band gap (3.37 eV), has attracted widespread attention due to its unique optical and electrical properties [4]. It has been applied in many fields, like transistor [5], photoluminescent [6], solar battery [7] and photocatalyst [8]. However, ZnO exhibits inherent defects involving poor photon absorption, low light utilization efficiency and high photoproduction electron-hole pairs recombination rate, which limits its applications. In order to overcome these disadvantages, one can integrate ZnO with other solid material to fabricate nanocomposite and thus to improve its performances [9,10].

In order to obtain nanocomposite, we can adhere one kind material to the surface of another substance with high specific area. In the past few years, some nanocomposites with interesting electronic and magnetic properties have been prepared via this method [11-13]. Cobalt selenide is a kind of semiconductor materials with band gap of 1.52 eV [14]. The varieties of cobalt selenide include CoSe [15,16], $CoSe_2$ [17] and $Co_{0.85}Se$ with nonintegral ratio [18-20]. In recent years, cobalt selenium has received extensive attention due to its excellent performances as catalyst in the fields of redox reaction, catalytic decomposition of hydrazine hydrate, magnetic refrigeration and Li-ion batteries [21,22]. CoSe nanoparticles have been synthesized by

microwave-assisted method or hydrothermal process, respectively [23,24]. Our research group has reported a type of graphene-like $Co_{0.85}Se$ nanosheets with good thermal and chemical stability properties [25]. This kind of nanosheets is considered as a good support for loading with metals and metal oxides, such as Fe_3O_4 [26]. The catalytic activities of oxides supported nanocomposites generally have been largely enhanced, which is attributed to the synergetic effect that occurs at the interface of oxide and selenide support. To the best of our knowledge, the nanocomposites from loading ZnO nanoparticles (ZnO NPs) on the surface of $Co_{0.85}Se$ nanosheets have not been reported so far.

With the development of the industrialization，water pollution is becoming more and more serious. Hydrazine hydrate is a kind of industrial pollutant with highly toxic [27]. The maximum permitted concentration of hydrazine is 0.01 mg/L for drinking water and its discharge standard is 0.1 mg/L. However, actual emissions have often exceeded this standard for many enterprises. p-nitrophenol (4-NP) is another toxic compound in the environment from manufacturing and processing of some industrial products [28,29]. Therefore, there is still a challenge for seeking a kind of catalyst with high efficient and low cost to remove hydrazine hydrate and 4-NP of waste water. Herein, we report the synthesis of a kind of ZnO-loaded $Co_{0.85}Se$ nanocomposites through a hydrothermal reaction, and explore its catalytic property for decomposition of hydrazine hydrate and hydrogenation reduction of 4-NP. After a series of characterizations, we found that freshly prepared ZnO NPs were well dispersed on the

surface of $Co_{0.85}Se$ nanosheets. Importantly, the obtained nanocomposites have higher catalytic performance for decomposition of hydrazine hydrate and hydrogenation reduction of 4-NP than either individual component of $Co_{0.85}Se$ nanosheets or ZnO NPs. Recycling experiments show that the nanocomposites have good repeatability and stability as catalyst for the decomposition of hydrazine hydrate. Thus, ZnO-loaded $Co_{0.85}Se$ nanocomposites could be potentially used as catalyst to remove hydrazine hydrate and 4-NP of polluted water.

2. Experimental section

2.1. Synthesis of ZnO-loaded $Co_{0.85}Se$ nanocomposites

The ZnO-loaded $Co_{0.85}Se$ nanocomposites were synthesized by a hydrothermal route. In a typical experiment, 0.146 g (0.5 mmol) $Co(NO_3)_2 \cdot 6H_2O$, 0.087 g (0.5 mmol) Na_2SeO_3 and 0.030 g (0.1 mmol) $Zn(NO_3)_2 \cdot 6H_2O$ were added into a teflon-lined stainless autoclave of 25 mL capacity in turns. Subsequently, 18 mL distilled water and 1.65 mL hydrazine hydrate (85%, wt%) were added into the autoclave under vigorous stirring. The solution was stirred vigorously for 20 min and then sealed and maintained at 140 ^oC for 24 h, and next cooled to room temperature naturally. The final black product was collected by centrifuging the reaction mixture and washed with distilled water and absolute ethanol respectively for three times and dried at 60 ^oC for 6 h for further characterization. In addition, individual $Co_{0.85}Se$ nanosheets

could be obtained without adding $Zn(NO_3)_2 \cdot 6H_2O$ to reaction system, and other experiment conditions were remained unchanged. ZnO NPs were synthesized via the method reported in previous our literature [30]. In addition, the compositions of nanocomposites are greatly influenced by amount of Zn sources, and related experiments have also been finished (see Supporting Information (SI), Figure S1-S2).

2.2. Catalytic experiments

2.2.1 The catalytic decomposition of hydrazine hydrate

We selected hydrazine hydrate as a model pollutant to investigate the catalytic activity of ZnO-loaded $Co_{0.85}Se$ nanocomposites. The catalytic experimentation was performed under the room temperature. The concentration of hydrazine hydrate was determined by the modified method as previous literature [26]. The color reagent is a mixture, including p-dimethylaminobenzaldehyde, 8 g; ethanol, 50.0 mL; concentrated hydrochloric acid (35 %, wt %), 50.0 mL.

We plotted a standard curve for determining the optimum concentration of hydrazine hydrate in the color development experiment. The details were as follows: Different volume of $2.0*10^{-3}$ M of hydrazine hydrate solutions was added to a 50 mL beaker with 2.5 mL color reagent, and the volume of mixture solution was maintained at 25 mL via replenishing distilled water. In order to form hydrazone compound, the mixture solution was placed at room temperature for 10 min. The concentration of

hydrazine was determined by UV-Vis absorbance of hydrazone mixture solution and calibration curve was drawn.

The reaction equation for hydrazine hydrate and color developing agent is described as follows:

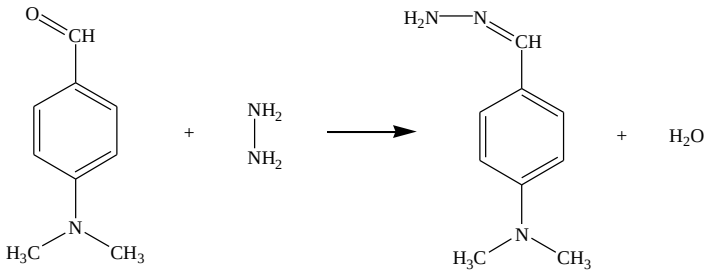

In catalytic experiments, 50 mg ZnO-loaded $Co_{0.85}Se$ nanocomposites and 100 mL of $2.0*10^{-3}$ M hydrazine hydrate solution was added into a 250 mL round bottom flask. To ensure a homogeneous temperature distribution during the hydrazine decomposition, the mixture was rapidly stirred at 25 ^{o}C in a water bath, then 2 mL mixed solution was taken out and centrifuged at different time intervals (2, 4, 6, 8, 10 and 12 min). After centrifugal separation, 0.5 mL supernatant and 2.5 mL chromogenic agent was placed in a beaker with 22.0 mL distilled water for chromogenic reaction at room temperature. After 10 min, 3 mL mixture solution was taken out for the measurement of UV-Vis spectrum

2.2.2 Catalytic hydrogenation of p-nitrophenol

The process of catalytic hydrogenation of 4-NP was explored in a standard quartz cuvette at room temperature [31, 32]. The exact catalytic process is as follows: firstly,

0.1 mL 4-NP aqueous solution (0.005 M) and 2 mL distilled water was mixed in a quartz cuvette, and the mixture solution emerged pale yellow. Then, after 1 mL freshly prepared aqueous solution of $NaBH_4$ (0.02 M) was also added to the quartz cuvette, the color of the solution changed to bright yellow rapidly because of the formation of p-nitrophenolate anion (4-NP ions). Secondly, 1 mg ZnO-loaded $Co_{0.85}Se$ nanocomposites as a catalyst were added into the quartz cuvette, and the color of the solution changed from bright yellow to colorless gradually. The catalytic process was monitored by a UV-vis spectrophotometer at 400 nm at constant time intervals. One can see that the intensity of the peak at 400 nm was gradually decreasing till disappearing [33-36].

3. Results and discussion

3.1. Characterization of ZnO-loaded $Co_{0.85}Se$ nanocomposites

The nanocomposites were synthesized via one step method under hydrothermal condition without using any surfactant. The composition and crystal phase purity of the synthesized product was first analyzed by the powder X-ray diffraction (XRD) technique. The XRD patterns of the samples were recorded in a 2θ range of 20^o-80^o.

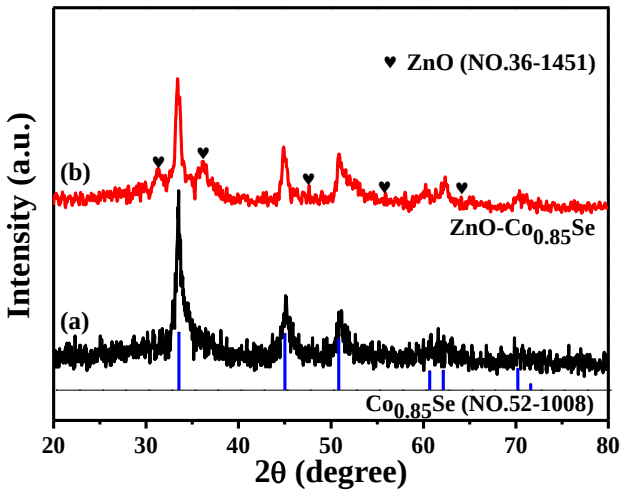

Figure 1. XRD patterns of the synthesized samples: (a) $Co_{0.85}Se$, (b) ZnO-loaded $Co_{0.85}Se$ nanocomposites.

Figure 1(a) shows the XRD patterns of the synthesized samples without Zinc source, and all diffraction peaks can be indexed to the phase of $Co_{0.85}Se$ hexagonal structure, which fits well with the standard data file of $Co_{0.85}Se$ (JCPDS 52-1008) [21]. No other impurity peaks were found from the XRD patterns. The XRD pattern of the typical product was shown in Figure 1(b). The diffraction peaks contain the characteristic peaks of $Co_{0.85}Se$ (JCPDS 52-1008) and the other peaks can be well indexed to hexagonal wurtzite ZnO (JCPDS 36-1451) [37]. XRD results show that the prepared particles are ZnO and $Co_{0.85}Se$ nanocomposites.

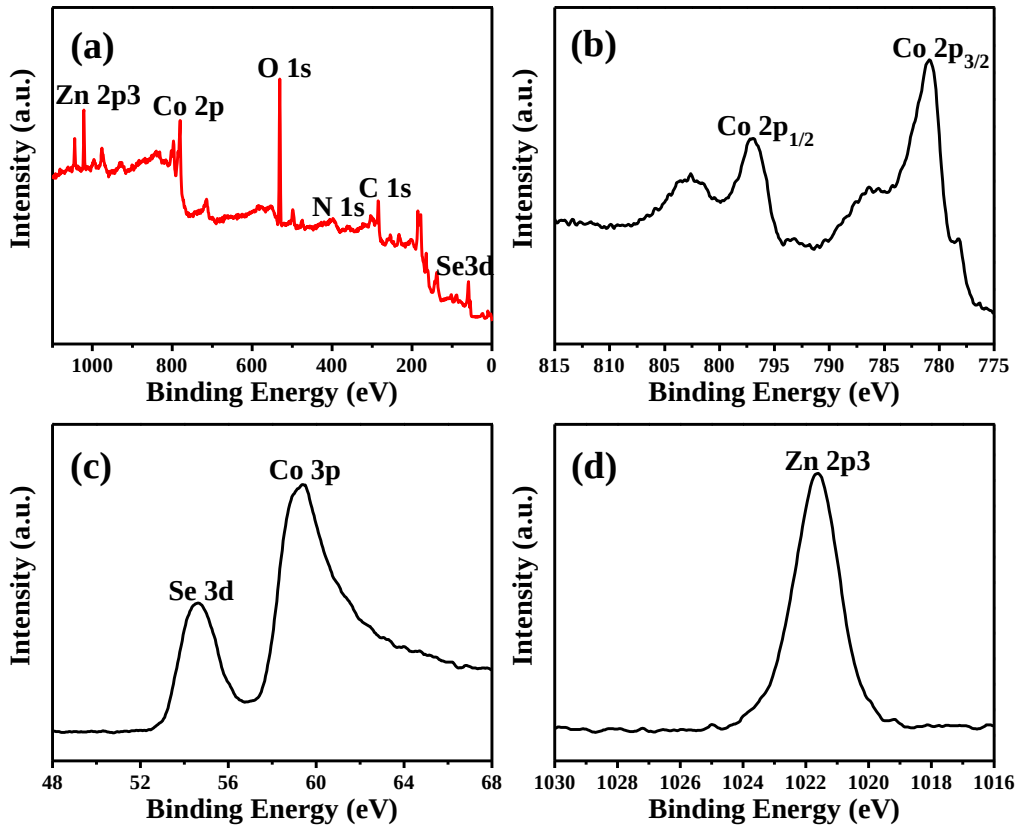

Figure 2. (a) XPS survey spectrum of ZnO-loaded $Co_{0.85}Se$ nanocomposites; (b), (c) and (d) are Co 2p, Se 3d and Zn 2p XPS spectra of the nanocomposites, respectively.

XPS survey spectrum of the synthesized samples is shown in Figure 2(a), which displays the peaks of C 1s (284.8 eV), N 1s (399.6 eV), O 1s (531.3 eV), Co 2p (781.0 eV), Se 3d (54.5 eV) and Zn 2p (1021.6 eV). To obtain more information about the samples, we performed high-resolution XPS spectra of Co, Se and Zn. From Figure 2(b), the binding energy of the Co $2p_{3/2}$ and Co $2p_{1/2}$ characteristic absorption peak occurs at 781.0 eV and 797.0 eV, respectively [38,39], while the peaks at 786.3 eV and 802.7 eV are secondary peaks of Co $2p_{3/2}$ and Co $2p_{1/2}$, respectively. The XPS result of Co demonstrates that the species of Co in the synthesized samples have two kinds of oxidation states including Co^{2+} and Co^{3+} [40,41]. The Figure 2(c) shows the

photoelectron peaks at 54.5 eV, 60.0 eV are characteristic absorption peak of Se $3d_{5/2}$ [42], Co 3p [43], respectively. The photoelectron peak occurs at 1021.63 eV is characteristic absorption peak of Zn $2p_{3/2}$, indicating that the Zn species exist in the form of Zn^{2+} in the ZnO-loaded $Co_{0.85}Se$ nanocomposites (Figure 2(d)). The XPS results further illustrate oxidation states of product, which is consistent with the characterization from the above XRD patterns.

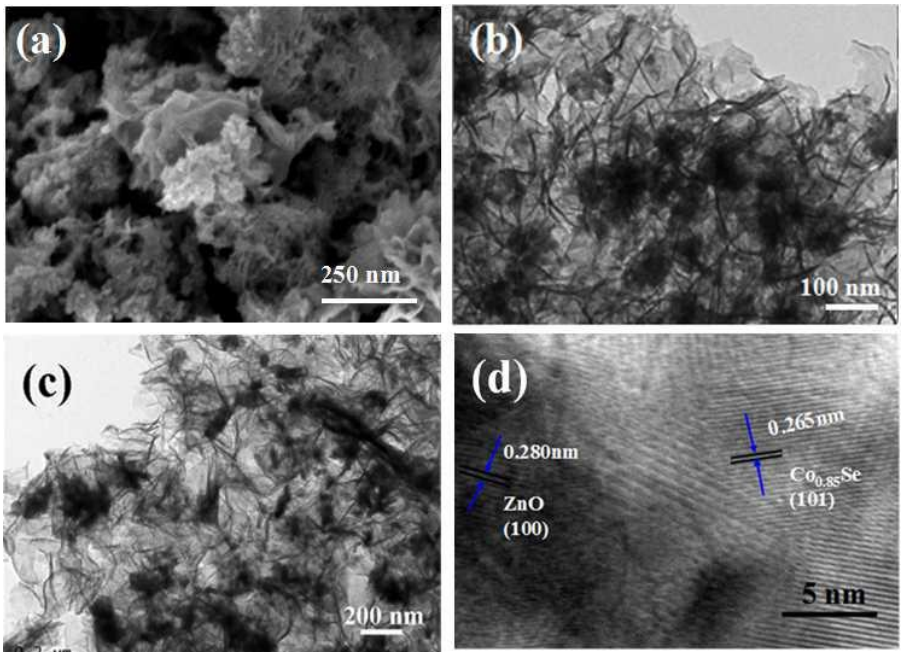

Figure 3. (a) SEM images of ZnO-loaded $Co_{0.85}Se$ nanosheets, (b, c) TEM images of ZnO-loaded $Co_{0.85}Se$, (d) HRTEM image of nanocomposites, respectively.

Figure 3(a) is SEM image of the obtained nanocomposites, in which shows that some NPs on the surface of the thin films. Figure 3(b) and 3(c) are TEM images of the obtained nanocomposites. We can see that the samples consist of thin films and NPs loaded on their surfaces. HRTEM image (Figure 3(d)) demonstrates that the d-spacing of 0.265 nm corresponds to (101) plane of hexagonal close-packed (hcp) $Co_{0.85}Se$,

while the d-spacing of 0.280 nm is in agreement with the (100) plane of hexagonal wurtzite phase ZnO. So the obtained nanocomposites are composed of $Co_{0.85}Se$ thin films and ZnO NPs attached on the surface of $Co_{0.85}Se$. All of these indicate that the synthesized samples are ZnO-loaded $Co_{0.85}Se$ nanocomposites. In order to provide detailed information about the shape of the $Co_{0.85}Se$ nanosheets and ZnO NPs, the SEM and TEM was tested (see SI, Figure S3).

3.2. BET measurement of the synthesized samples.

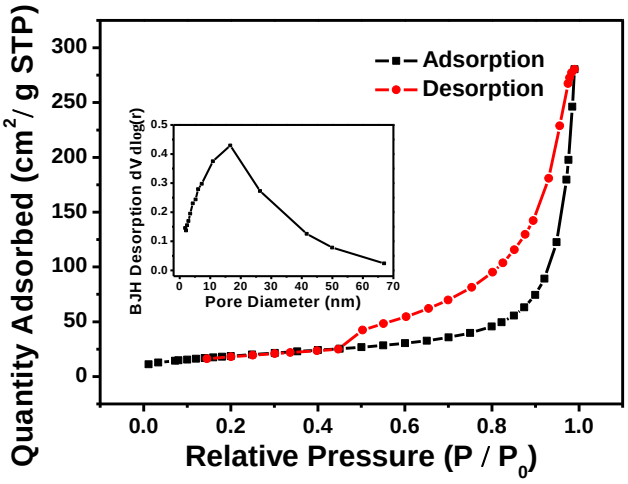

Figure 4. N_2 adsorption and desorption isotherm of ZnO-loaded $Co_{0.85}Se$ nanocomposites. The inset is the pore-size distribution curve.

Brunauer-Emmett-Teller (BET) measurement has been performed to analyze specific surface area and pore diameter of ZnO-loaded $Co_{0.85}Se$ nanocomposites. N_2 isotherms as shown in Figure 4 are close to Type IV curve with an evident hysteresis loop in the 0.45-1.0 range of relative pressure. BET specific surface area of the synthesized sample was calculated from N_2 isotherms at 77.5 K was 66.5 m^2 g^{-1}. The pore diameter was around 16.5 nm determined by Barrett-Joyner-Halenda (BJH)

method, which was attributed to the interparticles spaces. Compared with $Co_{0.85}Se$ nanosheets (55.1 m^2 g^{-1}), the high specific surface area of the ZnO-loaded $Co_{0.85}Se$ nanocomposites would provide more active sites for its adsorbent and catalytic behavior.

3.3. The catalytic decomposition of hydrazine hydrate

We find that the obtained ZnO-loaded $Co_{0.85}Se$ nanocomposites have high catalytic activity for decomposition of hydrazine hydrate. In acidic condition, the hydrazine hydrate can react with p-dimethylaminobenzaldehyde to form a yellow hydrazone with an absorption maximum at 456 nm. A standard curve was plotted between the mean absorbance for each standard concentration (X axis) and the target hydrazone concentration (Y axis). A representative standard curve is shown (see SI, Figure S4) and it reveals that there is a good linear relationship between the hydrazone absorbance and its concentration from $2.0*10^{-6}$ to $4.0*10^{-5}$ M. In the catalytic reaction, we added excess addition of chromogenic agent so that the concentration of generated hydrazone and the concentration of the rest of the hydrazine hydrate to conform to stoichiometric proportion (1:1). Thus, a good linear relationship is obtained between the absorbance value of hydrazone and the concentration of hydrazine hydrate. As a result, we can use p-dimethylaminobenzaldehyde as a probe molecule to monitor the decomposition of hydrazine hydrate.

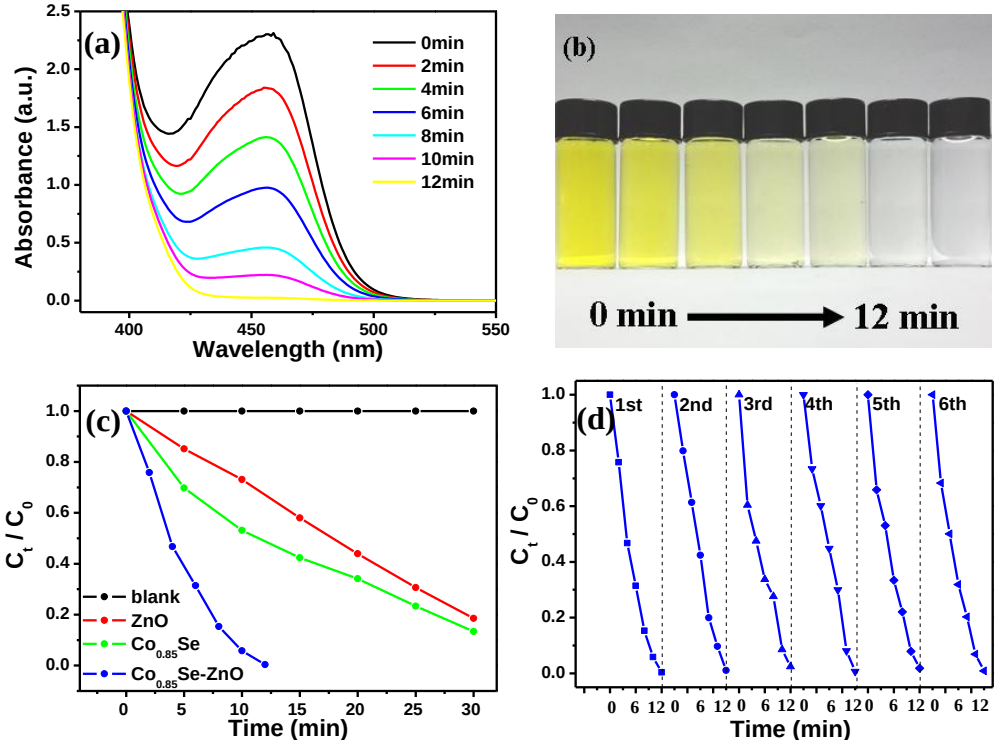

Figure 5. (a) UV-vis absorption spectra of the decomposition of hydrazine hydrate using ZnO-loaded $Co_{0.85}Se$ nanocomposites as catalyst; (b) the photos of the color change of the solution to the reaction time; (c) UV-vis absorption spectra of different catalysts for the decomposition of hydrazine hydrate; (d) Cycling runs of ZnO-loaded $Co_{0.85}Se$ nanocomposites for the decomposition of hydrazine hydrate.

In order to keep the hydrazone concentration within the linear range, we took 0.5 mL supernatant liquid of the mixture of ZnO NPs, $Co_{0.85}Se$ nanosheets, ZnO-loaded $Co_{0.85}Se$ nanocomposites and hydrazine hydrate at different time interval to react with color reagent for further UV-vis absorption spectra test, respectively. As shows in Figure 5(a), UV-vis absorption spectra tests show that the absorbance peak of hydrazone at 456 nm dropped rapidly along with the increase of reaction time and almost completely disappeared within 12 min. Figure 5(b) displayed that the corresponding color of the hydrazone solution changed from yellow to colorless with prolonging reaction time. UV-vis absorption spectra of ZnO NPs and $Co_{0.85}Se$ nanosheets as catalysts have been shown too (see SI, Figure S5). Figure 5(c) is

comparison diagram of different kind catalyst for catalytic decomposition of hydrazine hydrate in the same conditions. It demonstrated that there was no decomposition of hydrazine hydrate without any catalyst (Figure 5(c), black line). While in the presence of ZnO-loaded $Co_{0.85}Se$ nanocomposites, hydrazine hydrate could be completely degraded within 12 min (Figure 5(c) blue line). In contrast, the catalytic activities of pure $Co_{0.85}Se$ nanosheets and ZnO NPs for decomposition of hydrazine hydrate were low, and only 50% and 30% of hydrazine hydrate was decomposed for pure $Co_{0.85}Se$ nanosheets (Figure 5(c), green line), and ZnO NPs (Figure 5(c), red line) in the same time, respectively.

To evaluate catalytic stability and re-usability of ZnO-loaded $Co_{0.85}Se$ nanocomposites, we conducted recycling experiments for the decomposition of hydrazine hydrate under the same catalytic conditions. The decompose rate remains constant over 6 consecutive cycles, as shown in Figure 5(d), indicating the excellent stability and catalytic activity of ZnO-loaded $Co_{0.85}Se$ nanocomposites. The samples were collected after recycling experiments, centrifugal washing for XRD and TEM.

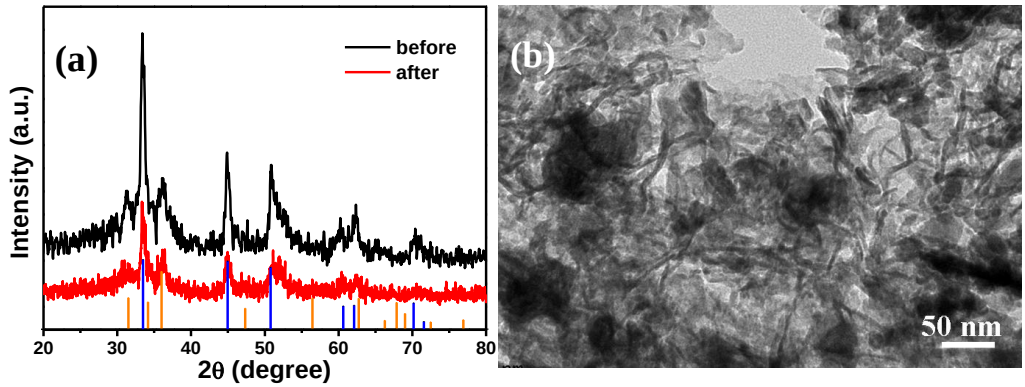

Figure 6. XRD pattern and TEM image of ZnO-loaded $Co_{0.85}Se$ nanocomposites after 6 consecutive cycles.

Figure 6(a) is the XRD patterns of the catalyst after 6 consecutive cycles. There is no difference of phase before and after the catalytic reaction. TEM image (Figure 6(b)) shows that $Co_{0.85}Se$ nanosheets have been damaged to some extent. The thin-film structure was curled or folded because the nanosheets could suffer from various external forces, such as centrifugation and stirring in the catalytic process. Though the morphology of sample slightly changed, its high catalytic activity was still kept during the catalyst was reused. Hence, the prepared ZnO-loaded $Co_{0.85}Se$ nanocomposites have stable performance as the catalyst for the decomposition of hydrazine hydrate.

Importantly, compared with current reports (Table 1), the prepared ZnO-loaded $Co_{0.85}Se$ nanocomposites presented best catalytic activity for catalytic decomposition of hydrazine hydrate (limited to the same measurement method for hydrazine hydrate).

Table 1

Comparison of the catalytic capacities of various catalysts reported in the literatures for the degradation of hydrazine hydrate.

Catalysts	Conversion efficiency retention	Initial concentrations of hydrazine hydrate (M)	time (min)	Amount of catalysts (mg mL^{-1})	Cycles	Ref.
$Co_{0.85}Se$/graphene hybrid nanosheets	97%	$2.0 * 10^{-3}$	12	0.5	10	21
tremelliform $Co_{0.85}Se$ nanosheets	95%	$2.0*10^{-3}$	50	0.5	6	25

cobalt selenide nanotubes	90%	$2.0*10^{-3}$	30	0.5	5	41
ZnO-loaded $Co_{0.85}Se$ nanocomposites	99%	$2.0*10^{-3}$	12	0.5	6	This work

3.4. Catalytic hydrogenation of p-nitrophenol

We found that the obtained ZnO-loaded $Co_{0.85}Se$ nanocomposites have efficient catalytic activity not only for decomposition of hydrazine hydrate but also for converting 4-NP to *p*-aminophenol (4-AP). Figure **7**(a) is the UV-vis absorption spectra of 4-NP before and after adding freshly prepared $NaBH_4$ solution. The pure 4-NP showed an absorption maximum at 317 nm, while the absorption peak converted redshift to 400 nm after $NaBH_4$ solution was added into the 4-NP aqueous solution. We can see that the color of the solution have shifted from pale yellow to bright yellow immediately after adding $NaBH_4$ solution (The inset in Figure 7(a)). Figure 7(b) is the UV-vis absorption spectra of adding freshly prepared $NaBH_4$ into 4-NP solution in the absence of catalyst, after 30 min, the absorbance value of the solution decreased less, which illustrates that the reaction rate of the hydrogenation reaction of 4-NP to 4-AP is very low without catalyst.

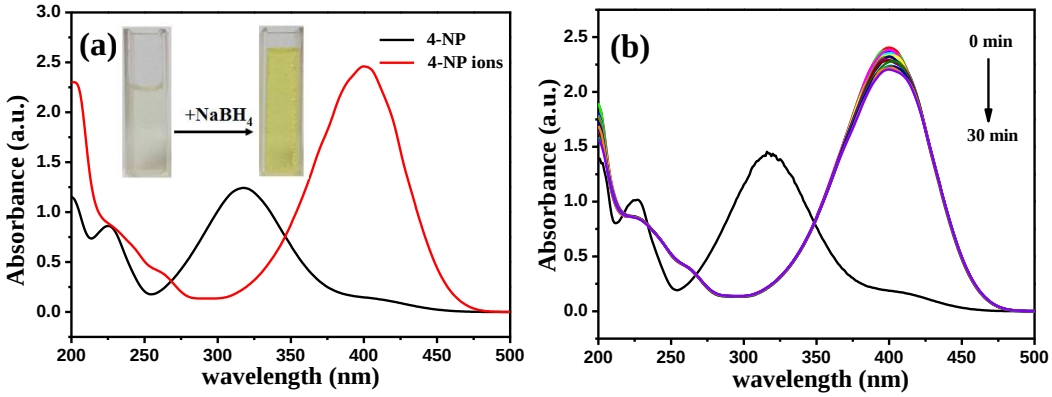

Figure 7. UV-vis absorption spectra: (a) of 4-NP and 4-NP ions after adding $NaBH_4$ solution, (the inset is photo of 4-NP and 4-NP ion solution) and (b) 4-NP ions in the absence of catalyst. Conditions: [4-NP] = 0.005 M; [$NaBH_4$] = 0.02 M, 25 °C.

Figure 8(a-c) shows UV-vis spectra of the sample in the presence of different kind catalysts. When 1.0 mg of ZnO NPs as a catalyst was added into the reactive system, the absorption peak at 400 nm has no obvious decrease with time increasing (Figure 8(a)). Figure 8(b) shows the UV-vis absorption spectra for the same mass of the $Co_{0.85}Se$ nanosheets as the catalyst, and the conversion of 4-NP within 20 min could be finished 95%. It's worth noting that the conversion of 4-NP could be completely catalyzed within 10 min, which is much faster than that of the $Co_{0.85}Se$ nanosheets and ZnO NPs, if using the same mass of the ZnO-loaded $Co_{0.85}Se$ nanocomposites as the catalyst (Figure 8(c)). Figure 8(d) displays the natural logarithmic plots of absorbance at 400 nm against reaction time with $Co_{0.85}Se$ nanosheets and ZnO-loaded $Co_{0.85}Se$ nanocomposites.

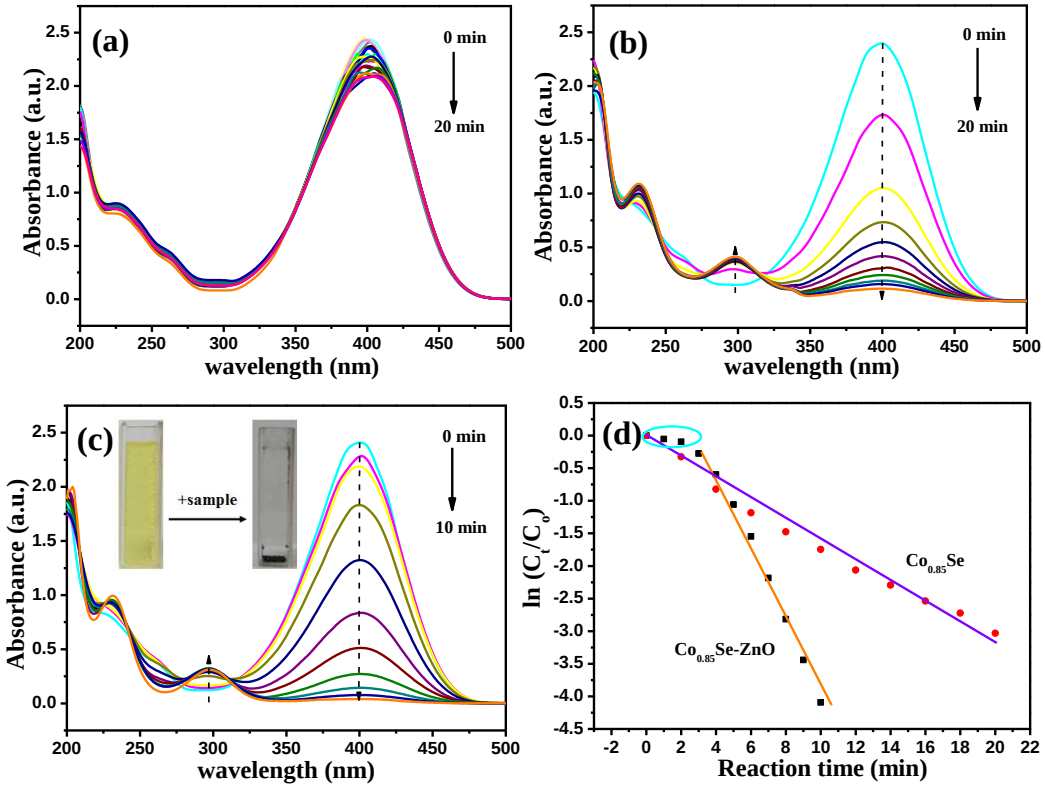

Figure 8. Time dependent absorption spectra for the catalytic reduction of 4-NP by $NaBH_4$ in the presence of 1 mg catalyst: (a)ZnO NPs, (b) $Co_{0.85}Se$ nanosheets, (c) ZnO-loaded $Co_{0.85}Se$ nanocomposites. (d) The relationships of ln (C_t /C_0) versus reaction time plot in presence of 1 mg different catalysts. Conditions: [4-NP] = 0.005 M, [$NaBH_4$] = 0.02 M, 25 °C.

The good linear correlation indicates the reaction could follow the kinetic equation ln (C_t / C_0)=ln (A_t /A_0) = -kt (the concentrations of 4-NP at time t and 0 are donated as C_t and C_0, and the absorbance of 4-NP at time t and 0 are defined as A_t and A_0) [44,45]. Encircled data points shows a certain period of time required for the reactant molecules to adsorb onto the surface of catalyst before the reaction could be initiated, which is called as induction time [46-48]. We found that the time of catalytic reaction reduced with increasing amount of ZnO-loaded $Co_{0.85}Se$ nanocomposites in the catalytic process, and the catalytic efficiency was improved (see SI, Figure S6).

Compared with current reports (Table 2), the prepared ZnO-loaded $Co_{0.85}Se$ nanocomposites presented a better catalytic activity for catalytic hydrogenation of

p-nitrophenol than other non-noble metal nanocatalysts.

Table 2

Comparison of the catalytic capacities of non-noble metal nanocatalysts reported in the literatures for the hydrogenation of p-nitrophenol.

catalysts	Initial concentrations of 4-NP (M)	Amount of catalysts (mg)	time (min)	Conversion efficiency retention	Ref.
Co/Ti film	$2.0* 10^{-4}$	2 cm × 5 cm film	16	93%	49
$Co_{0.85}Se$ bundle-like nanostructure	$5.0* 10^{-4}$	1	10	100%	50
$NiCo_2$ Alloys	$1.0 * 10^{-4}$	1	30	100%	51
ZnO-loaded $Co_{0.85}Se$ nanocomposites	$5.0* 10^{-2}$	1	10	100%	This work

3.5. Electrochemical impedance spectroscopy of samples

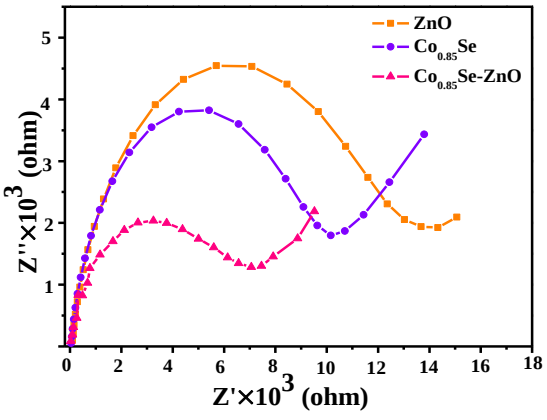

Figure 9. EIS Nyquist plots of ZnO, $Co_{0.85}Se$ and ZnO-loaded $Co_{0.85}Se$ nanocomposites electrodes. Conditions: $[K_3[Fe(CN)_6]]$ = 0.004 M; [Sample] = 0.5 mg/mL; the frequency range is between 0.1 Hz and 100 KHz with signal amplitude of 5 mV.

Electrochemical impedance spectroscopy (EIS) may well be taken to indicate the

rate of interfacial charge transfer of materials. Figure 9 shows the EIS response spectra of ZnO, $Co_{0.85}Se$ and ZnO-loaded $Co_{0.85}Se$ nanocomposites. The radius of the arc on the EIS Nynquist plot reflects the reaction rate occurring at the surface of electrode, in which the smaller radius of materials, faster transfer rate of electron. Obviously, the ZnO-loaded $Co_{0.85}Se$ nanocomposites possess smallest the radius of EIS Nynquist plot among three samples, and next is $Co_{0.85}Se$ nanosheets, ZnO NPs, in that order. Thus is totally consistent with above catalytic effect for decomposition of hydrazine hydrate in Figure 5(c) and catalytic hydrogenation of p-nitrophenol in Figure 8(d).

4. Conclusion

In summary, a new kind of ZnO-loaded $Co_{0.85}Se$ nanocomposites have been successfully prepared through a facile, effective, and scalable hydrothermal method. Electron microscope images show that the ZnO NPs were homogeneously attached on the surface of $Co_{0.85}Se$ nanosheets. The BET surface area of obtained nanocomposites reached 66.5 $m^2 g^{-1}$, which is higher than that of pure $Co_{0.85}Se$ nanosheets (55.1 $m^2 g^{-1}$) and ZnO NPs (11.54 $m^2 g^{-1}$). The phase and morphology of the prepared products were greatly influenced by mole number of Zn sources, and the optimal Zn sources is 0.1 mmol $Zn(NO_3)_2 \cdot 6H_2O$ in our synthesis system. Interestingly, the as-prepared ZnO-loaded $Co_{0.85}Se$ nanocomposites exhibit excellent catalytic activity and reusability for decomposition of hydrazine hydrate in aqueous solution and reduction

of p-nitrophenol at room temperature, and 100 mL of $2.0*10^{-3}$ M hydrazine hydrate solution can be decomposed in 12 min with 50 mg obtained nanocomposites. This catalytic efficiency is the highest one in current literatures. The result can be attributed to high specific surface area and interfacial effect of nanocomposites. Therefore, ZnO-loaded $Co_{0.85}Se$ nanocomposites can be potential used as catalysts to remove hydrazine hydrate of wastewater and catalytic hydrogenation of 4-NP.

Acknowledgements

This work is supported by the National Science Foundation of China (NSFC) (Grants 21471001, 21275006), and Natural Science Foundation of Anhui Province (Grant no.1508085MB22), Financed by the 211 Project of Anhui University, and The Key Laboratory of Functional Inorganic Materials Chemistry of Anhui Province.

References

[1] S. K. Arya, C. C. Wong, Y. J. Jeon, et al, Chem. Rev. 115 (2015) 5116-5158.

[2] E. Fortunato, P. Barquinha, R. Martins, Adv. Mater. 24 (2012) 2945-2986.

[3] B. Neppolian, Q. L. Wang, H. Yamashita, et al, Appl. Catal. A 333 (2007) 264-271.

[4] Z.Y. Fan, D.W. Wang, P. C. Chang, et al, Appl. Phys. Lett. 85 (2004) 5923-5925.

[5] D. Rothenstein, B. Claasen, B. Omiecienski, et al, J. Amer. Chem. Soc. 134 (2012) 12547-12556.

[6] C. H. Chia, W. C. Tsai, W. C. Chou, J. Lumin. 148 (2014) 111-115.

[7] J. B. Baxter, A. M. Walker, K. V. Ommering, et al, Nanotechnology 17 (2006) S304-S312.

[8] T. J. Kuo, C. N. Lin, C. L. Kuo, et al, Chem. Mater. 19 (2007) 5143-5147.

[9] C. Zhang, J. Zhang, Y. J. Su, et al, Physica E 56 (2014) 251-255.

[10] D. L. Li, W. H. Wu, Y. P. Zhang, et al, J. Mater. Sci. 49 (2014) 1854-1860.

[11] J. Su, M. H. Cao, L. Ren, et al, J. Phys. Chem. C 115 (2011) 14469-14477.

[12] Y. Y. Li, J. Q. Liu, H. Q. Dong, et al, Nanotechnology 25 (2014) 065602-065611.

[13] L. Xu, Y. G. Wei, W. Guo, et al, Appl. Surf. Sci. 332 (2015) 682-693.

[14] W. R. Liyanage, S. Mishra, K. Song, et al, RSC Adv. (2014) 28140-28147.

[15] P. Nekooi, R. Ahmadi, M. K. Amini, J. Indian Chem. Soc. 9 (2012) 715-722.

[16] Y. Q. Lai, F.Y. Liu, J. Yang, et al, Appl. Phys. Express 4 (2011) 070201.

[17] L. Zhu, M. Teo, P.C. Wong, et al, Appl. Catal. A 386 (2010) 157-165.

[18] Y. K. Liu, F.Y. Liu, C. Huang, et al, Mater. Lett. 108 (2013) 110-113.

[19] J. Dong, J. H. Wu, M. Zheng, et al, J. Mater. Sci-Mater. Electron 26 (2015) 2501-2507.

[20] J. F. Zhao, J. M. Song, C. C. Liu, et al, CrystEngComm 13 (2011) 5681-5684.

[21] L. F. Zhang, C.Y. Zhang, Nanoscale 6 (2014) 1782-1789.

[22] Y. J. Feng, T. He, N. Alonso-Vante, Electrochim. Acta 54 (2009) 5252-5256.

[23] P. Nekooi, M. Akbari, M. K. Amini, Inter. J. Hydrogen Energy 35 (2010) 6392-6398.

[24] X. H. Liu, N. Zhang, R. Yi, et al, Mater. Sci. Eng. B 140 (2007) 38-43.

[25] C. C. Liu, J. M. Song, J. F. Zhao, et al, Appl. Catal. B 119-120 (2012) 139-145.

[26] J. M. Song, S. S. Zhang, S. H. Yu, Small 10 (2014) 717-724.

[27] R. Kaveeshwar, V. K. Gupta, Fresenius J, Anal. Chem. 344 (1992) 114.

[28] C. M. Fan, L. F. Zhang, S. S. Wang, et al, Nanoscale, 4 (2012) 6835-6840.

[29] G. Q. Gao, L. Lin, C. M. Fan, Q. Zhu, et al, J. Mater. Chem. A, 1 (2013) 12206-12212.

[30] J. M. Song, J. Zhang, J. J. Ni, H. L. Niu, C. J. Mao, S. Y. Zhang, Y. H. Shen, CrystEngComm 16 (2014) 2652-2659.

[31] S. Bai, X. P. Shen, G. X. Zhu, M. Z. Li, H.T. Xi, K. M. Chen, ACS Appl. Mat. Interfaces 4 (2012) 2378-2386.

[32] Z. F. Jiang, D. L. Jiang, A. M. S. Hossain, K. Qian, J. M. Xie, Phys. Chem. Chem. Phys. 17 (2015) 2550-2559.

[33] R. Xu, H. P. Bi, G. Y. He, J. W. Zhu, H. Q. Chen, Mater. Res. Bull.57 (2014)190-196.

[34] Y. G. Wu, M. Wen, Q. S. Wu, H. Fang, J. Phys. Chem. C 118 (2014) 6307-6313.

[35] H. L. Yang, S. W. Li, X. Y. Zhang, X. Y. Wang, J. T. Ma, J. Mater. Chem. A 2 (2014) 12060-12067.

[36] F. H. Lin, R. A. Doong, Appl. Catal. A 486 (2014) 32-41.

[37] S. S. Yi, J. B. Cui, S. Li, et al, Appl. Surf. Sci. 319 (2014) 230-236.

[38] L. Predoana, A. Jitianu, M. Voicescu, et al, J. Sol-Gel Sci. Technol. 74 (2015) 406-418.

[39] N. Naveen, S. Selladurai, Physica B 457 (2015) 251-262.

[40] J. F. Marco, J. R. Gancedo, M, Gracia, et al, J. Mater. Chem. 11 (2001) 3087-3093.

[41] Z. H. Wang, S. Qiang, F.W. Zhang, et al, CrystEngComm 5 (2013) 5928-5934.

[42] Q.S. Jiang, G. Hu, Mater. Lett. 153 (2015) 114-117.

[43] Z. Y. Zhang, S. P. Pang, H. X. Xu, et al, RSC Adv. 3 (2013) 16528-16533.

[44] A. Bhattacharjee, M. Ahmaruzzaman, Mater. Lett. 157 (2015) 260-264.

[45] H. Feng, T. T. ThanhThuy, L. Chen, L. J. Yuan, Q. Y. Cai, Chem. Eng. J. 215 (2013) 591-599.

[46] P. P. Shanbogh, S. C. Peter, RSC Adv. 3 (2013) 22887-22890.

[47] S. Sarkar, L. Balisetty, Pradeep P. Shanbogh, Sebastian C. Peter, J. Catal. 318 (2014)143-150.

[48] S. Wunder, F. Polzer, Y. Lu, Y. Mei and M. Ballauff, J. Phys. Chem. C, 114 (2010) 8814-8820.

[49] H. Li, J. Y. Liao, T. Zeng, Catal. Sci. Technol. 4 (2014) 681-687.

[50] Z. X. Zhang, X. W. Wang, K. L. Wu, et al, New J. Chem. 38 (2014) 6147-6151.

[51] K. L. Wu, X. W. Wei, X. M. Zhou, D. H. Wu, et al, J. Phys. Chem. C 115 (2011) 16268-16274.

Graphical Abstract

A kind of ZnO-loaded $Co_{0.85}Se$ nanocomposites have been successfully synthesized via one pot route without using any surfactant or structure-directing agents. The obtained nanocomposites exhibit remarkable catalytic performance for the decomposition of hydrazine hydrate and catalytic hydrogenation of p-nitrophenol at room temperature.